ELSEVIER

Catalysis Today 72 (2002) 205–211

CATALYSIS TODAY

www.elsevier.com/locate/cattod

Low-temperature catalytic growth of carbon nanotubes under microwave plasma assistance

Xizhang Wang, Zheng Hu*, Qiang Wu, Yi Chen

Laboratory of Mesoscopic Materials Science, Department of Chemistry, Nanjing University, Nanjing 210093, PR China

Abstract

Various carbon nanotubes (CNTs) including aligned arrays, Y-branching and some other novel morphologies have been catalytically grown on anodic porous alumina template (APAT) and on the alumina-supported catalysts with methane (*or benzene*) as carbon source under microwave plasma assistance below 520 °C. The growth process could be simply operated since neither heating nor bias-voltage was applied to the catalysts or APAT. The results presented in this paper not only greatly richened the nanostructures of carbon family but also provided with a new technique path for synthesizing CNTs or some other nanostructures with the characteristics of low-temperature which has some special advantages or applications.

Keywords: Carbon nanotubes; Microwave plasma; Chemical vapor deposition; Alumina template; Array; Y-branching

1. Introduction

Carbon nanotubes (CNTs) have shown unmatched physical and chemical properties [1,2], e.g. high mechanical strength [3] and peculiar electrical properties [4,5], which might lead to a variety of new important applications such as the reinforcing elements in composites [6], electron field emitters [7–9], chemical sensors [10], hydrogen and electric power storages [11,12], molecular transistors [13,14], and nanodevices [15]. These promising applications have provided the impetus for the international, multi-disciplinary studies on CNTs in the past few years. Of course, the growth of CNTs is a prerequisite either for basic scientific researches or for practical applications. To date, many methods have been developed to synthesize the CNTs. Paying attention to the synthesis temperature, it is found that most methods were operated at high-temperature over 4000 °C, e.g. for graphite arc-discharge and laser vaporization [16,17], or moderate-temperature around 1000 °C, e.g. for catalytic growth through decomposition of hydrocarbons [18,19], and little is known about the low-temperature synthesis of CNTs, i.e. below 700 °C, due to the difficulty to activate the chemical reaction. Obviously, it is very important to develop the low-temperature synthesis of CNTs either for research interests or for practical importance. For example to integrate CNTs with electronic device, the synthesis temperature must be far below 660 °C, i.e. the melting point of aluminum, because most electric connections are made of aluminum. For the promising use as cold cathode flat panel displays, it is desirable to grow CNT emitters perpendicular to the surface of display glass while the strain point of the best display glass is only 666 °C [20]. Such kind of challenges have promoted the exploration of low-temperature synthesis of CNTs. It is well known that “active” and “low-temperature”

* Corresponding author. Tel.: +86-25-3592909 (O); fax: +86-25-3317761.
E-mail address: zhenghu@netra.nju.edu.cn (Z. Hu).

0920-5861/02/$ – see front matter
PII: S0920-5861(01)00494-1

are two important characteristics of non-equilibrium plasma [21]. Consequently, the synthesis temperature could be greatly decreased by catalytic growth under plasma assistance. Recently, it was reported that aligned CNT arrays could be grown on nickel deposited glass by a hot filament plasma-enhanced chemical vapor deposition (PECVD) below 660 °C [20,22] and very late, aligned CNT arrays on APAT were synthesized by electron cyclotron resonance chemical vapor deposition (ECR-CVD) even at ∼100 °C by applying a −300 V dc bias-voltage [23].

Microwave plasma operating at low pressure is another kind of low-temperature plasma due to the non-equilibrium state between electrons and other heavy particles in plasma space, and is full of active species. In this paper, we reported a catalytic growth of various carbon nanostructures on the metal (Fe, Co and/or Ni) catalysts supported on γ-alumina carrier or the aligned CNT arrays and Y-branching CNTs on the APAT with methane (*or benzene*) as carbon source below 520 °C under microwave plasma assistance. The experiments could be operated in a rather simple way since neither heating nor bias-voltage was applied to the catalysts or APAT.

2. Experimental

2.1. Preparation of the supported catalysts

The preparation procedure of the metal (Fe, Co and/or Ni) catalysts supported on γ-alumina is briefly described as follows. As an example, an Fe/γ-Al_2O_3 catalyst containing 2.88 mmol Fe per gram of γ-Al_2O_3 was prepared by impregnating 5.00 g γ-Al_2O_3 powder (specific surface area: 212 m^2/g) with 7.00 ml water solution containing 14.4 mmol $Fe(NO_3)_3{\cdot}9H_2O$ (analytical reagent). The impregnation typically lasted for 24 h at ambient temperature until drying. The material was then dried at 110 °C for 3 h, sintered at 500 °C for 3 h, followed by grinding into 40 mesh particles. This resulting catalyst was denoted as 2.88 mmol/g Fe/γ-Al_2O_3.

2.2. Fabrication of anodic porous alumina template (APAT)

A typical process for forming APAT is described as follows: APAT with the channel diameters of 30–50 nm and pore interval of ca. 70 nm was fabricated by anodizing an aluminum sheet (99.5%) in 20 wt.% sulfuric acid solution at 0 °C under 20 V, which self-organized into a highly ordered hexagonal close-packed array of parallel vertically oriented pores. Followed by the electrochemical plating, Ni nanoparticles as catalyst were deposited at the bottoms of the template nanochannels. For Y-branching APAT, the fabrication process is similar to that in literature [24]. By regulating the anodizing voltage, the type and concentration of electrolyte, as well as the anodizing temperature and time, various APAT parameters such as the pore sizes, pore depths, pore intervals, and internal pore structures (branching or not) could be fabricated.

2.3. Growth of carbon nanostructures, CNT arrays, and Y-branching CNTs

Approximate 20 mg supported catalyst or a ca. 5 mm × 5 mm size of APAT with aluminum substrate was placed into a quartz tube, with an inner diameter of 30 mm, that was vertically placed and connected between vacuum system and inlet of the mixture of hydrogen, argon, and methane (*or benzene* carried by argon gas). The mixture gases were led into the system on the top of the quartz tube and the flux of the mixture gases were monitored by a digital mass flowmeter. The total pressure in the chamber during synthesis was kept constant in the range from 1.0×10^3 to 5.0×10^4 Pa measured by a Pirani vacuum gauge. The microwave generator operated at 2.45 GHz was continuously variable with the maximum output of 800 W. The alumina-supported catalysts or the APAT in all experiments were placed in plasma zone where the growth of carbon nanostructures occurred. To estimate the temperature in the growth zone, a piece of hard glass with strain point of 520 °C was loaded close to the catalysts as a probe. The supported catalysts or the APAT were first pre-treated by *hydrogen and argon* plasma for 20 or 5 min and followed by the addition of CH_4 for the growth of carbon nanostructures for 30 or 60 min, respectively. The typical flux of hydrogen, argon and methane were 20, 67 and 3.5 ml/min, respectively in case of supported catalysts, while the flux of methane was replaced by 7 ml/min in case of APAT, with the system pressure of 1.0×10^3 and 2.0×10^3 Pa

correspondingly. The typical incident microwave powder was 360 W.

2.4. Products characterization techniques

All TEM observations were carried out with a JEOL-JEM-1005 transmission electron microscopy (TEM) operated at 100 kV. The samples for TEM experiments were dispersed in ethanol–water solution (50% v/v) under ultrasonic treatment for ca. 10 min and then transferred to a copper grid with polymer membrane. For the as-grown samples containing APAT, the templates were first removed using condensed hydrochloric acid and then TEM observations were performed. The specimens for scanning electron microscopy (SEM) observations were first evaporated a platinum film and then SEM observations were carried out with a JEOL-JSM-6300 SEM.

3. Results

3.1. TEM studies of carbon nanostructures on the alumina-supported catalysts

The results from TEM observations indicated that the diameters of CNTs obtained on supported catalysts ranged from 6 to 60 nm, and the lengths were up to 20 μm. Fig. 1 gives the TEM patterns of some typical configurations of carbon nanostructures on different supported catalysts. Fig. 1a shows the ordinary morphology of multi-walled CNTs with the diameters of ca. 10 nm, which is analogous to those obtained by thermal CVD. Fig. 1b gives the bamboo-like CNTs with ca. 18 nm diameters. The CNT in Fig. 1c looks like a snail with the gradually increasing radii. The interesting morphologies of the planar spiral, helix-shaped and cone-tower-like CNTs are shown in Fig. 1d–f, respectively. The diameter of the CNT in Fig. 1g becomes smaller and smaller gradually, partially filled with the catalyst inside the inner hole. A ribbon-like carbon nanostructure shown in Fig. 1h looks like that the CNT was crushed. The CNTs in Fig. 1i and j are full of defects, with relatively large empty or partially filled inner space. The CNTs in Fig. 1k looks like pigtails, while those in Fig. 1l are partially filled carbon nanoparticles.

It should be noted that for all these experiments, no deformation has been observed for the hard glass probe, in other words, the growth temperature of CNTs was lower than 520 °C. From above description, it is learned that various morphologies of CNTs could be catalytically grown with different catalysts and synthesis parameters under microwave plasma assistance at low-temperature (below 520 °C). In addition to the ordinary morphologies, several novel ones have been observed, which richened the family of CNTs. Some morphologies are very attractive. For example, the abundance of defects and large inner space for the CNTs in Fig. 1i may be beneficial to hydrogen storage or some other purposes. However, in most cases, only a mixture of CNTs with different morphologies could be obtained by using γ-Al_2O_3 supported catalysts. Therefore, in the following part, we used APAT to constrain the growth of CNTs.

3.2. SEM/TEM studies on CNT arrays

Aligned CNT arrays are especially interesting due to the great important in developing novel functional devices. If CNT array could be catalytically grown inside the APAT below 660 °C, the aluminum substrate of APAT could then act as electrode directly for field emission, which is, of course, very attractive and is also what we would like to do.

Fig. 2 is SEM/TEM images of the APAT and CNT arrays/bundles. Fig. 2a is the TEM image of our APAT with the channel diameters in 30–50 nm and pore interval of ca. 70 nm. Fig. 2b shows the SEM micrograph of the as-grown template-containing CNT array observed from the side view. It can be seen that those straight tubes are parallel to and isolated with each other. In order to learn more detailed information about the product, TEM image was obtained for the sample after removing the APAT by using condensed hydrochloric acid as a chemical etchant. Due to the van de Waals interaction among the CNTs [25], the aligned pattern has not been totally destroyed and the CNT bundles can still be seen clearly as shown in Fig. 2c and d. The nanotubes are straight with the lengths of ca. 4 μm and diameters of ca. 40 nm. Fig. 2e and f give the TEM patterns of the CNT bundles from two APATs with different pore sizes, pore depths, and pore intervals. The diameters and the lengths of CNTs shown in Fig. 2e and f are ca. 50 nm and 1 μm, 60 nm

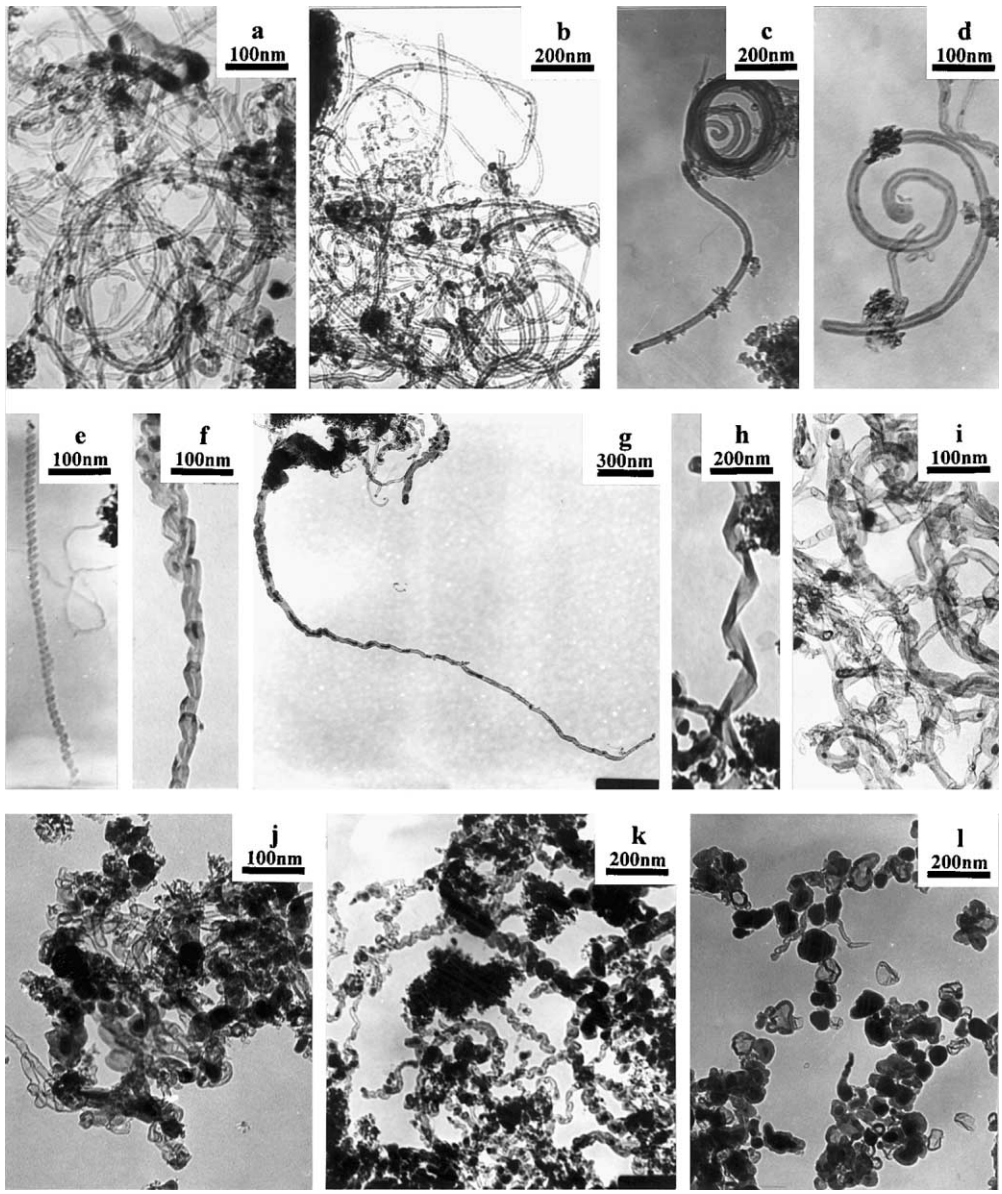

Fig. 1. TEM patterns of some typical configurations of carbon nanostructures on various alumina-supported catalysts (a) ordinary configurations of CNTs; (b) bamboo-like CNTs; (c) snail-like CNT; (d) a planar spiral CNT; (e) a helix-shaped CNT; (f) a cone-tower-like CNT; (g) a CNT with variable diameter partially filled with catalyst; (h) a ribbon-like carbon nanostructure; (i) large inner space thin-walled CNTs; (j) short thin-walled CNTs and carbon nanoparticles partially filled with catalyst; (k) pigtail-like CNTs; (l) carbon nanoparticles partially filled with catalyst. Note: The specific synthesizing paramenters including the catalyst, the flux of working gases and the incident microwave power are listed below, respectively, (a) 2.88 mmol/g Fe/γ-Al_2O_3, H_2:Ar:CH_4 = 20:67:3.5(ml/min), 280 W; (b) 1.36 mmol/g Ni/γ-Al_2O_3, H_2:Ar:CH_4 = 5:67:3.5 (ml/min), 280 W; (c) 2.88 mmol/g Ni/γ-Al_2O_3, H_2:Ar (C_6H_6) = 20:67 (ml/min), 280 W; (d) 2.88 mmol/g Fe/γ-Al_2O_3, H_2:Ar:CH_4 = 10:67:7 (ml/min), 280 W; (e) 2.88 mmol/g Ni/γ-Al_2O_3, H_2:Ar(C_6H_6) = 20:67 (ml/min), 280 W; (f) 1.47 mmol/g Fe-1.40 mmol/g Ni/γ-Al_2O_3, H_2:Ar:CH_4 = 20:67:3.5 (ml/min), 360 W; (g) 2.90 mmol/g Co/γ-Al_2O_3, H_2:Ar(C_6H_6) = 20:29 (ml/min), 360 W; (h) 2.88 mmol/g Fe/γ-Al_2O_3, H_2:Ar:CH_4 = 20:67:3.5 (ml/min), 520 W; (i) 2.88 mmol/g Fe/γ-Al_2O_3, H_2:Ar:CH_4 = 5:67:7 (ml/min), 280 W; (j) 2.88 mmol/g Fe/γ-Al_2O_3, H_2:Ar:CH_4 = 5:67:2 (ml/min), 360 W; (k) 1.44 mmol/g Fe-0.82 mmol/g Co-0.69 mmol/g Ni/γ-Al_2O_3, H_2:Ar:CH_4=20:67:3.5 (ml/min), 360W; (l) 2.88 mmol/g Fe/γ-Al_2O_3, H_2:Ar:CH_4 = 5:67:10 (ml/min), 280 W.

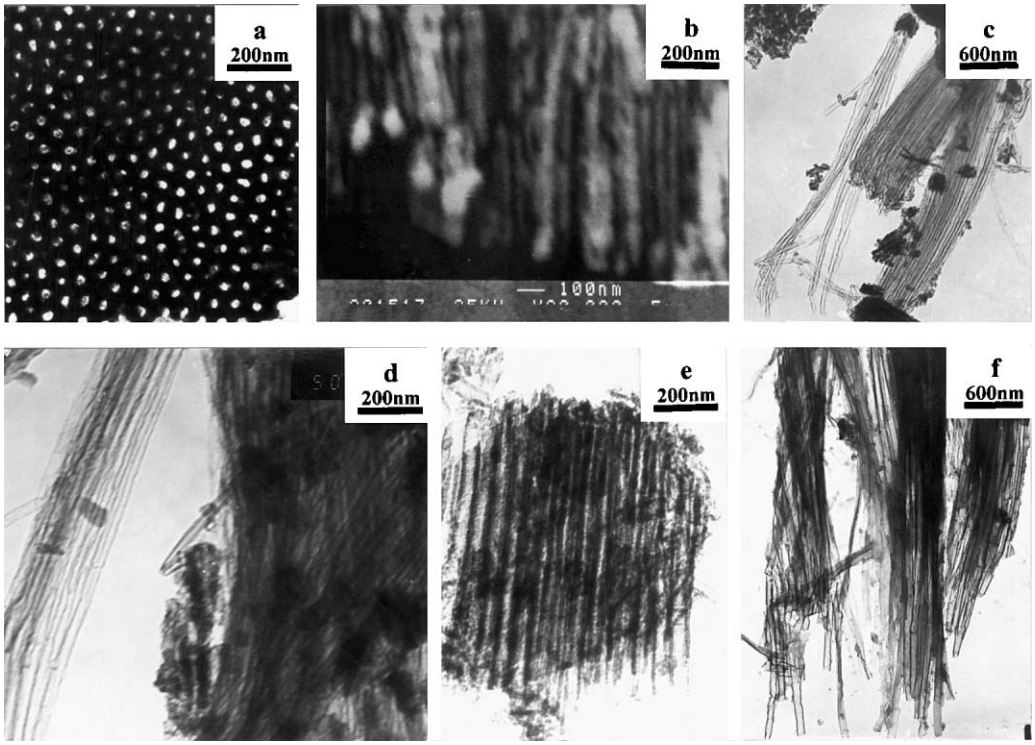

Fig. 2. SEM/TEM images of the APAT and CNT arrays/bundles (a) TEM image of APAT; (b) SEM micrograph of as-grown CNT array on APAT; (c)–(f) TEM patterns of CNT bundles after the removal of APATs with different parameters. The flux of hydrogen, argon and methane were 20, 67 and 7 ml/min, respectively, the pressure was 2.0×10^3 Pa, and the incident microwave powder was 360 W.

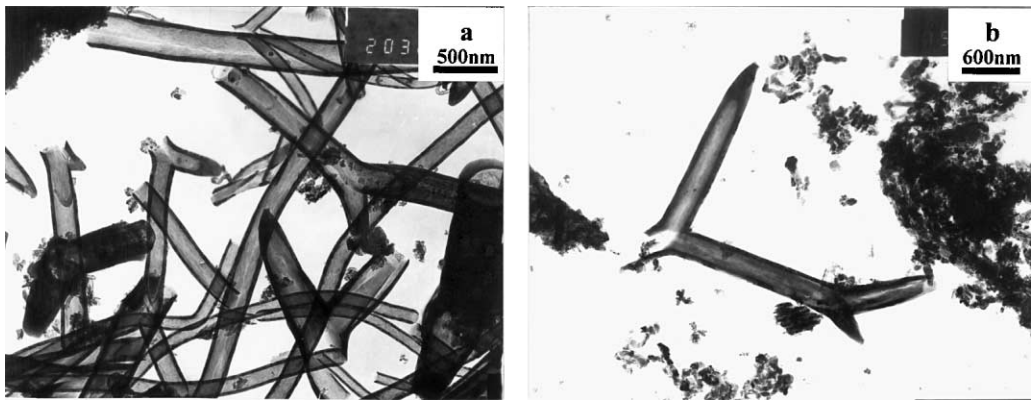

Fig. 3. TEM images of Y-branching CNTs with conic offshoots. The flux of hydrogen, argon and methane were 20, 67 and 7 ml/min, respectively, the pressure was 2.0×10^3 Pa, and the incident microwave powder was 360 W.

and 6 μm, respectively. These results indicate that the characteristics of CNT arrays, e.g. diameters, lengths, and densities, could be controlled by regulating the corresponding parameters of APATs, which, in turn, were determined by anodization parameters.

3.3. TEM studies on Y-branching CNTs

With the constraint of highly ordered APAT, aligned CNT arrays have been catalytically grown under plasma assistance at low-temperature. Furthermore, with the constraint of branched APAT, Y-branching CNTs have also been catalytically synthesized at low-temperature, which is of importance for the development of CNT-based electric devices and circuits. Fig. 3 shows the TEM images of the Y-branching CNTs, with the diameter of ca. 250 nm. The offshoots almost have a conic structure. Actually, this kind of huge hollow Y-branching CNTs have never been reported before, thereby, rather scientifically interesting.

4. Discussion and conclusions

Some striking features in this study are worth noting. Firstly, under microwave plasma assistance, catalytic growth of CNTs could be performed at rather low-temperature (below 520 °C) which is crucial for growing CNTs on the substrate with low-deforming temperature. Several novel morphologies have been obtained by this method. Secondly, by regulating the parameters of APAT such as the pore sizes, pore depths, pore intervals, and internal pore structures (branching or not), which is easily adjustable through, e.g. the anodizing voltage and time, the type and concentration of electrolyte, as well as the anodizing procedure and temperature, it is feasible to control the parameters of CNT arrays or Y-branching CNTs. Thirdly, CNT arrays and Y-branching CNTs synthesized by this method is not inherently area limited and can be scaled up with the template size. Furthermore, neither heating nor bias-voltage should be applied to the supported catalysts or APAT, which made the fabrication process operate easily. Finally, due to the “active” characteristic in plasma space, plasma-assisted catalytic growth is not only suitable for synthesizing CNTs but also for some other novel systems. Actually, BN nanotube arrays have already been synthesized in our lab similarly. From above description, it is seen that the whole fabrication process is reliable, inexpensive, and productive. These advantages are very important for both fundamental researches and future practical applications.

The growth mechanisms of carbon nanotubes by catalytic growth have been proposed as either base- or tip-growth on catalysts [26,27]. According to the TEM results in Fig. 1, the catalysts are seldom found on the top of CNTs obtained on the alumina-supported catalysts, which implies that the growth of CNTs in these cases follows the base-growth mechanism. On the contrary, the growth of CNTs on APAT keeps to the tip-growth mechanism and the porous alumina template itself may act as a catalyst, otherwise the Y-branching CNTs would not be formed. Actually, in our additional experiments, CNT arrays could also be produced even without depositing the catalyst at the bottoms of the template nanochannels. Therefore, it is reasonable to regard that the carbon species firstly deposited on the catalyst at the bottom of template nanochannels acted as seeds and then the CNTs were confined to grow within the APAT nanochannels through APAT self-catalysis. The synergism of “catalytic activation” and “plasma activation” in our case makes it possible to grow CNTs at temperature lower than that in normal catalytic growth through decomposition of hydrocarbons where only “catalytic activation” exists.

In summary, various CNTs including aligned arrays, Y-branching and some other novel morphologies have been catalytically grown on APATs and on the alumina-supported catalysts with methane (*or benzene*) as carbon source under microwave plasma assistance below 520 °C. Neither heating nor bias-voltage was needed to apply to the catalysts or APATs during growing process. These results not only greatly richened the nanostructures of carbon family but also provided with a new technique path for synthesizing CNTs or some other nanostructures with the characteristics of low-temperature, which has some special advantages or applications.

Acknowledgements

The authors greatly acknowledge financial support from NSFC, “973” program (G1999064508),

Hua-Ying Foundation of Nanjing University, as well as Visiting Scholar Foundation of Key Lab in University.

References

[1] P.M. Ajayan, S. Iijima, Nature 361 (1993) 333.
[2] J. Tersoff, R.S. Ruoff, Phys. Rev. Lett. 73 (1994) 676.
[3] M.M.J. Treacy, T.W. Ebbesen, J.M. Gibson, Nature 381 (1996) 678.
[4] J.W. Mintmire, B.I. Dunlap, C.T. White, Phys. Rev. Lett. 68 (1992) 631.
[5] N. Hamada, S. sawada, A. Oshiyama, Phys. Rev. Lett. 68 (1992) 1579.
[6] P.M. Ajayan, L.S. Schadler, C. Giannaris, A. Rubio, Adv. Mater. 12 (2000) 750.
[7] W.A. de Heer, A. Châtelain, D. Ugarte, Science 270 (1995) 1179.
[8] S.S. Fan, M.G. Chapline, N.R. Franklin, T.W. Tombler, A.M. Cassell, H.G. Dai, Science 283 (1999) 512.
[9] H. Murakami, M. Hirakawa, C. Tanaka, H. Yamakawa, Appl. Phys. Lett. 76 (2000) 1776.
[10] J. Kong, N.R. Franklin, C.W. Zhou, M.G. Chaplin, S. Peng, K. Cho, H.D. Dai, Science 287 (2000) 622.
[11] G.L. Che, B.B. Lakshmi, E.R. Fisher, C.R. Martin, Nature 393 (1998) 346.
[12] C. Liu, Y.Y. Fan, M. Liu, H.T. Cong, H.M. Cheng, M.S. Dresselhaus, Science 286 (1999) 1127.
[13] S.J. Tans, A.R.M. Verschuern, C. Dekker, Nature 393 (1998) 49.
[14] S. Frank, P. Poncharal, Z.L. Wang, W.A. de Heer, Science 280 (1998) 1744.
[15] P.G. Collins, A. Zettl, H. Bando, A. Thess, R.E. Smally, Science 278 (1997) 100.
[16] S. Iijima, Nature 354 (1991) 56.
[17] S. Iijima, T. Wakabayashi, Y. Achiba, J. Phys. Chem. 100 (1996) 5839.
[18] M. José-Yacamán, M. Miki-Yoshida, L. Rendón, J.G. Santiesteban, Appl. Phys. Lett. 62 (1993) 657.
[19] Z.W. Pan, S.S. Xie, B.H. Chang, C.Y. Wang, L. Lu, W. Liu, W.Y. Zhou, W.Z. Li, Nature 394 (1998) 631.
[20] Z.F. Ren, Z.P. Huang, J.W. Xu, J.H. Wang, P. Bush, M.P. Siegal, P.N. Provencio, Science 282 (1998) 1105.
[21] X.Z. Wang, Q. Wu, Z. Hu, H. Xu, S. Miao, Y. Chen, Plasma Sci. Technol. 2 (2000) 405.
[22] Z.F. Ren, Z.P. Huang, D.Z. Wang, J.G. Wen, J.W. Xu, J.H. Wang, L.E. Calvet, J. Chen, J.F. Klemic, M.A. Reed, Appl. Phys. Lett. 75 (1999) 1086.
[23] S.H. Tsai, F.K. Chiang, T.G. Tsai, F.S. Shieu, H.C. Shih, Thin Solid Films 366 (2000) 11.
[24] J. Li, C. Papadopoulos, J. Xu, Nature 402 (1999) 253.
[25] R.S. Ruoff, J. Tersoff, D.D.C. Lorents, S. Subramoney, B. Chan, Nature 364 (1993) 514.
[26] R. Stöckel, K. Janischowsky, M. Stammler, L. Ley, M. Albrecht, H.P. Strunk, Diamond Relat. Mater. 7 (1998) 147.
[27] L.C. Qin, D. Zhou, A.R. Krauss, D.M. Gruen, Appl. Phys. Lett. 72 (1998) 3437.